

## THERMAL BEHAVIOUR OF SOME NICKEL(II)–MORPHOLINE COMPLEXES

*J. Gálvez, J. Palazón, G. López and G. García*

DEPARTMENT OF INORGANIC CHEMISTRY, UNIVERSITY OF MURCIA,  
MURCIA, SPAIN

(Received December 5, 1983)

The preparation of  $\text{Ni}(\text{CN})_2 \cdot 1.5\text{M}$  (M = morpholine) and the thermal study of this and  $\text{NiBr}_2 \cdot 3\text{M}$ ,  $\text{NiI}_2 \cdot 4\text{M}$  and  $\text{Ni}(\text{NCS})_2 \cdot 4\text{M}$  are described. The thermal treatment of these compounds leads to the isolation of  $\text{Ni}(\text{CN})_2 \cdot \text{M}$ ,  $\text{Ni}(\text{CN})_2 \cdot 0.5\text{M}$ ,  $\text{NiBr}_2 \cdot 2\text{M}$ ,  $\text{NiI}_2 \cdot 3\text{M}$ ,  $\text{NiI}_2 \cdot 1.5\text{M}$ ,  $\text{Ni}(\text{NCS})_2 \cdot 2\text{M}$  and  $\text{Ni}(\text{NCS})_2 \cdot \text{M}$ . With the exception of  $\text{NiBr}_2 \cdot 2\text{M}$  and  $\text{Ni}(\text{NCS})_2 \cdot 2\text{M}$ , all intermediate species are reported here for the first time. Magnetic and spectral studies have been carried out to determine the mode of coordination and stereochemistry of the complexes. The thermal study includes the determination of stability, apparent activation energy and reaction orders, and reaction enthalpies.

In a recent paper [1] the authors reported on the preparation and study of some nickel complexes of the type  $\text{NiX}_2 \cdot \text{M}_n$  [M = morpholine; X =  $\text{C}_6\text{F}_5$  ( $n = 2$ ),  $\text{NO}_3$  ( $n = 3$ ), Br ( $n = 2, 3$ ) and I ( $n = 4$ )]. The use of the dehydrating agent 2,2-dimethoxypropane was shown to be a decisive factor in the preparation of some of these complexes. On the other hand, the investigation of the nickel thiocyanate–morpholine system led to the isolation of compounds  $\text{Ni}(\text{NCS})_2 \cdot \text{M}_n$  ( $n = 4, 2$ ) [2].

Although morpholine usually acts as a unidentate N-donor ligand in its complexes with nickel [1–4], it is a potentially bidentate (O- and N-donor) ligand. The thermal treatment of metal complexes containing morpholine can give rise to vacant coordination sites, which can in turn be occupied by the O-donor end of morpholine, the ligand thereby acting as a bridging group.

Here we describe the preparation of  $\text{Ni}(\text{CN})_2 \cdot 1.5\text{M}$  and the thermal study of this and  $\text{NiBr}_2 \cdot 3\text{M}$ ,  $\text{NiI}_2 \cdot 4\text{M}$  and  $\text{Ni}(\text{NCS})_2 \cdot 4\text{M}$ . The thermal study includes the determination of stability, kinetic parameters such as apparent activation energy and reaction order, and reaction enthalpies.

### Experimental

#### *Materials*

Morpholine and 2,2-dimethoxypropane were obtained from May and Baker Ltd. and Fluka, respectively, and used as such. Nickel salts were commercial products.

### Analyses

C, H, N analyses were performed with a Perkin–Elmer 240C microanalyzer. Nickel was determined by titration with EDTA [5].

### Physical measurements

Infrared spectra were recorded in Nujol mulls in the range 4000–250  $\text{cm}^{-1}$  on a Perkin–Elmer 457 spectrophotometer. The diffuse reflectance spectra were recorded in Nujol mulls on a Beckman DK-2A spectrophotometer; the mulls were smeared between two glass plates on filter paper and run against a reference consisting of similar plates containing Nujol only. Thermal decomposition studies were carried out in nitrogen on a Netzsch STA-429 thermobalance;  $\text{Al}_2\text{O}_3$  was used as reference material. Magnetic susceptibilities were measured by the Faraday method using a Cahn RG 2102 electrobalance and a Systron Conner 6001 electromagnet calibrated with  $\text{Co}[\text{Hg}(\text{SCN})_4]$  [6].

### Preparation of the nickel complexes

$\text{NiBr}_2 \cdot 3\text{M}$  and  $\text{NiI}_2 \cdot 4\text{M}$  were prepared as described in [1], while  $\text{Ni}(\text{NCS})_2 \cdot 4\text{M}$  was prepared according to indications from Ahuja and Singh [2]. For the preparation of  $\text{Ni}(\text{CN})_2 \cdot 1.5\text{M}$  the following experimental procedure was used: a suspension of 0.58 g of anhydrous  $\text{Ni}(\text{CN})_2$  [7] in 5 ml of 2,2-dimethoxypropane was refluxed for 1/2 h, then 5 ml of morpholine was added and the yellow-brown colour changed to light violet. After stirring for 12 h, the solid was filtered off under  $\text{N}_2$  and washed with diethyl ether. Although the product was dried under vacuum, its IR spectrum revealed the presence of traces of water. Yield 84%. The analytical data on this compound are given in Table 1.

**Table 1** Colours and analytical data of nickel compounds

Compound	Colour	Analysis, %, found (calcd.)			
		C	H	N	Ni
$\text{Ni}(\text{SCN})_2 \cdot \text{M}$	green-grey	27.1 (27.5)	3.9 (3.4)	17.7 (16.1)	
$\text{Ni}(\text{CN})_2 \cdot 1.5\text{M}$	pale violet	38.7 (39.8)	5.8 (5.6)	20.6 (20.3)	24.5 (24.3)
$\text{Ni}(\text{CN})_2 \cdot \text{M}$	bluish violet	35.6 (36.4)	4.5 (4.5)	19.9 (21.2)	
$\text{Ni}(\text{CN})_2 \cdot 0.5\text{M}$	blue	30.8 (31.1)	3.3 (2.9)	20.2 (22.7)	
$\text{NiI}_2 \cdot 3\text{M}$	green	25.4 (25.1)	5.0 (4.7)	6.9 (7.3)	
$\text{NiI}_2 \cdot 1.5\text{M}$	deep green	17.3 (16.2)	3.9 (3.1)	4.7 (4.7)	

## Results and discussion

### Thermal behaviour

Figure 1 shows the DTA and TG curves obtained for  $\text{NiBr}_2\cdot 3\text{M}$ ,  $\text{NiI}_2\cdot 4\text{M}$ ,  $\text{Ni}(\text{CN})_2\cdot 1.5\text{M}$  and  $\text{Ni}(\text{NCS})_2\cdot 4\text{M}$  under dynamic nitrogen atmosphere. These thermal curves were recorded with a heating rate of 5 deg/min, but those used for the determination of reaction orders and activation energies were recorded with a heating rate of 2 deg/min in order to achieve greater accuracy. Both theoretical and experimental weight losses are given in Table 2, along with their corresponding reactions, temperature ranges, and temperatures at the peaks in the DTA curves.

$\text{NiBr}_2\cdot 3\text{M}$  (I). This brownish compound is stable up to  $80^\circ$ ; the first stage of decomposition takes place between  $80$  and  $182^\circ$ . In this stage one mole of M is released to give  $\text{NiBr}_2\cdot 2\text{M}$  (II). The process is endothermic, with a DTA peak at  $172^\circ$ . Compound II is an isolable, blue solid, which decomposes slowly and non-regularly between  $182$  and  $365^\circ$  to give finally  $\text{NiBr}_2$ . The DTA curve shows three endothermic peaks, at  $227$ ,  $252$  and  $270^\circ$ .

$\text{NiI}_2\cdot 4\text{M}$  (III). Under  $\text{N}_2$  this compound shows a first decomposition stage between  $50$  and  $127^\circ$ , in which a weight loss occurs corresponding to 1 mol of morpholine per formula unit to yield  $\text{NiI}_2\cdot 3\text{M}$  (IV). In this stage two partially overlapping endothermic peaks are observed at  $110$  and  $115^\circ$ , possibly attributed to the decomposition of III and the fusion of IV, respectively. In fact, IV is obtained as a viscous liquid which solidifies on cooling. Compound IV decomposes between  $127$  and  $185^\circ$ , giving

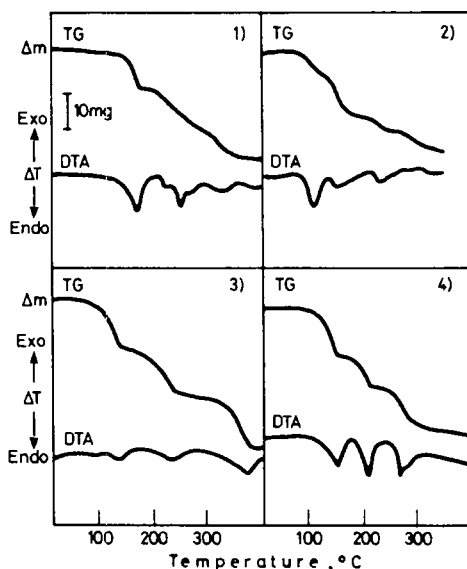


Fig. 1 Simultaneous TG and DTA curves of thermal decomposition in  $\text{N}_2$  of: 1)  $\text{NiBr}_2\cdot 3\text{M}$ , 88.0 mg; 2)  $\text{NiI}_2\cdot 4\text{M}$ , 58.9 mg; 3)  $\text{Ni}(\text{CN})_2\cdot 1.5\text{M}$ , 74.2 mg; and 4)  $\text{Ni}(\text{NCS})_2\cdot 4\text{M}$ , 47.9 mg

Table 2 Data on decomposition of compounds NiX<sub>2</sub>nM

Decomposition reaction	Weight loss, in percent		Temperature range, °C(TG)	DTA peaks	Activation energy, kJ mol <sup>-1</sup>	Reaction order
	Theoretical	Experimental				
NiBr <sub>2</sub> 3M(I) → NiBr <sub>2</sub> 2M(II) + M	18.1	19.4	80–192	172	115.8	0.5
NiBr <sub>2</sub> 2M(II) → NiBr <sub>2</sub> + 2M	36.3	32.8 *	182–365	227 252 270	—	—
NiI <sub>2</sub> 4M(III) → NiI <sub>2</sub> 3M(IV) + M	13.2	13.0	50–127	110 115	—	—
NiI <sub>2</sub> 3M(IV) → NiI <sub>2</sub> 1.5M(V) + 1.5M	19.8	21.4	127–185	152	—	—
NiI <sub>2</sub> 1.5M(V) → NiI <sub>2</sub> + 1.5M	19.8	17.7	214–332	230	—	—
Ni(CN) <sub>2</sub> 1.5M(VI) → Ni(CN) <sub>2</sub> M(VII) + 0.5M	18.0	17.6	60–143	103 140	73.9	0.5
Ni(CN) <sub>2</sub> M(VII) → Ni(CN) <sub>2</sub> 0.5M(VIII) + 0.5M	18.0	17.6	143–245	240	80.0	0.5
Ni(CN) <sub>2</sub> 0.5M(VIII) → Ni(CN) <sub>2</sub> + 0.5M	18.0	19.2	290–385	378	159.5	0.5
Ni(NCS) <sub>2</sub> 4M(IX) → Ni(NCS) <sub>2</sub> 2M(X) + 2M	33.3	32.1	105–159	153	134.0	0.5
Ni(NCS) <sub>2</sub> 2M(X) → Ni(NCS) <sub>2</sub> M(XI) + M	16.6	16.7	175–217	212	183.4	1
Ni(NCS) <sub>2</sub> M(XI) → Ni(NCS) <sub>2</sub> + M (decomposes)	—	—	235–304	270 279	—	—

\* The weight loss continues slowly.

$\text{NiI}_2\text{1.5M}$  (V). However, it should be noted that at  $185^\circ$  the TG curve is not a horizontal line, and compound V decomposes progressively and non-regularly to yield  $\text{NiI}_2$  (at  $332^\circ$ ). The overall weight loss (52.1%) is close to the theoretical one (52.7%).

$\text{Ni(CN)}_2\text{1.5M}$  (VI). This pale violet compound, which is stable up to  $60^\circ$ , decomposes through three stages well discernible in the TG curve. In the first stage (between  $60$  and  $143^\circ$ ) it loses 0.5 M to give  $\text{Ni(CN)}_2\text{M}$  (VII); in the second stage the weight loss corresponds to 0.5 M (in the range  $143$ – $245^\circ$ ) and  $\text{Ni(CN)}_2\text{0.5M}$  (VIII) is formed. An additional loss of 0.5 M leads finally to the formation of  $\text{Ni(CN)}_2$ . Compounds VII and VIII are isolable solids.

$\text{Ni(NCS)}_2\text{4M}$  (IX). This compound is stable up to  $105^\circ$ . Between  $105$  and  $159^\circ$  the loss of 2 M occurs through a well defined stage to give  $\text{Ni(NCS)}_2\text{2M}$  (X). This result is in agreement with the information from Ahuja and Singh, who obtained  $\text{Ni(NCS)}_2\text{2M}$  by heating  $\text{Ni(NCS)}_2\text{4M}$  in an air oven at *ca.*  $120^\circ$  [2]. Compound X loses a further molecule of neutral ligand in the range  $175$ – $217^\circ$ . The compound obtained in this stage,  $\text{Ni(NCS)}_2\text{M}$  (XI), loses morpholine and decomposes from  $235^\circ$ . However, the observed weight loss is larger than that expected for one molecule of morpholine, because the release of morpholine is overlapped by the decomposition of  $\text{Ni(NCS)}_2$ . Endothermic peaks are observed at  $153$ ,  $212$ ,  $270$  and  $279^\circ$  in the DTA curve.

Analytical data on the isolated intermediates are collected in Table 1.

### Structural study

Here we consider only the compounds  $\text{NiI}_2\text{3M}$ ,  $\text{NiI}_2\text{1.5M}$ ,  $\text{Ni(NCS)}_2\text{M}$  and the 1:1.5, 1:1 and 1:0.5  $\text{Ni(CN)}_2$ -morpholine compounds, because all other complexes have been studied previously [1, 2]. The magnetic moments and electronic spectral data are given in Table 3.

**Table 3** Magnetic moments and electronic spectra of nickel complexes

Compound	$\mu_{\text{eff}}(\text{BM})^*$	Electronic bands ( $\text{cm}^{-1}$ )
$\text{Ni(SCN)}_2\text{M}$	3.10	9.660, 16.390
$\text{Ni(CN)}_2\text{1.5M}$	2.40	11.430, 17.605
$\text{Ni(CN)}_2\text{M}$	2.16	11.365, 17.515
$\text{Ni(CN)}_2\text{0.5M}$	2.20	10.050, 16.980
$\text{NiI}_2\text{3M}$	3.91	8.700, 14.600
$\text{NiI}_2\text{1.5M}$	3.76	12.270, 15.750, 17.700

\* At  $20^\circ$ ; diamagnetic corrections were made.

Both the electronic spectrum and magnetic moment of  $\text{NiI}_2\text{3M}$  can be interpreted by assuming pseudooctahedral geometry for the compound. The bands at  $8700\text{ cm}^{-1}$  and  $14600\text{ cm}^{-1}$  can be assigned to the transition from the ground state  $^3\text{A}_{2g}(\text{F})$  to the excited states  $^3\text{T}_{2g}(\text{F})$  ( $\nu_1$ ) and  $^3\text{T}_{1g}(\text{F})$  ( $\nu_2$ ), respectively. The structural situation of the nickel atom would be similar to that observed in  $\text{NiBr}_2\text{3M}$  [1], for which the presence of bidentate morpholine was reported.

The electronic spectrum of  $\text{NiL}_21.5\text{M}$  shows a single band at  $12270\text{ cm}^{-1}$  and a double band with maxima located at  $15750\text{ cm}^{-1}$  and  $17700\text{ cm}^{-1}$ , which can be interpreted by assuming a pseudotetrahedral environment for the nickel atom. In fact, the spectrum is similar to those observed for pseudotetrahedral complexes of the type  $\text{NiX}_2\text{L}_2$  [8]. On this basis, the band at  $12270\text{ cm}^{-1}$  is assigned as  $\nu_2\ 3\text{T}_1(\text{F}) \rightarrow 3\text{A}_2(\text{F})$  and the bands at  $15750$  and  $17700\text{ cm}^{-1}$  as components from  $\nu_3\ 3\text{T}_1(\text{F}) \rightarrow 3\text{T}_1(\text{P})$ . The magnetic moment (3.76 BM) found for this compound also supports the tetrahedral stereochemistry, as it is in the 3.5–4.0 BM range generally observed for fairly tetrahedral complexes [9]. The assignment of tetracoordinated nickel in  $\text{NiL}_21.5\text{M}$  requires that either iodide or morpholine acts as a bridging ligand; there is indeed infrared spectral evidence (see below) that some morpholine is O-bonded to nickel.

The  $\text{Ni}(\text{CN})_2$ -morpholine system resembles the  $\text{Ni}(\text{CN})_2\text{-H}_2\text{O}$  and  $\text{Ni}(\text{CN})_2\text{-NH}_3$  systems [10]. Thus, the magnetic moments of the three compounds,  $\text{Ni}(\text{CN})_2x\text{M}$  (2.40, 2.16 and 2.20 BM for  $x = 1.5, 1$  and  $0.5$ , respectively) and the presence of absorptions in the infrared spectra at  $2160, 560\text{--}555, 490\text{--}480$  and  $440\text{ cm}^{-1}$ , identified as  $\nu(\text{CN}), \nu(\text{Ni-CN}), \nu(\text{Ni-NC})$  and  $\delta(\text{NiCN})$  [11], respectively, allow us to assign a structure consisting of layers of composition  $\text{Ni}(\text{CN})_2$ ; each  $\text{Ni}^{2+}$  would be surrounded by either the carbon ends or the nitrogen ends of four  $\text{CN}^-$  ions. Each  $\text{Ni}^{2+}$  ion in a  $\text{NiN}_4$  unit would complete a *trans*-octahedral coordination with morpholine molecules coordinated via the N atom, this accounting for the stoichiometry  $\text{Ni}(\text{CN})_2\text{M}$ . The 1:1 ratio of octahedrally and planar coordinated  $\text{Ni}^{2+}$  ions in  $\text{Ni}(\text{CN})_2\text{M}$  satisfactorily accounts for the observed magnetic moment, since the former are paramagnetic and the latter diamagnetic. The remaining morpholine in  $\text{Ni}(\text{CN})_21.5\text{M}$  may well occupy gaps in the layer structure, since there is infrared evidence of the presence of uncoordinated morpholine. In contrast, the infrared spectrum of  $\text{Ni}(\text{CN})_20.5\text{M}$  is compatible with the presence of bridging morpholine. The two bands observed in the diffuse reflectance spectra of these compounds (Table 3) are also consistent with the proposed structures and can be interpreted as  $\nu_1\ 3\text{A}_{2g}(\text{F}) \rightarrow 3\text{T}_{2g}(\text{F})$  and  $\nu_2\ 3\text{A}_{2g}(\text{F}) \rightarrow 3\text{T}_{1g}(\text{F})$ , respectively.

From a consideration of the magnetic moment (3.10 BM) and the electronic spectrum,  $\text{Ni}(\text{NCS})_2\text{M}$  is suggested to have  $\text{Ni}^{2+}$  ions in an octahedral environment. The electronic bands at  $9660$  and  $16390\text{ cm}^{-1}$  can be assigned as  $\nu_1\ 3\text{A}_{2g}(\text{F}) \rightarrow 3\text{T}_{2g}(\text{F})$  and  $\nu_2\ 3\text{A}_{2g}(\text{F}) \rightarrow 3\text{T}_{1g}(\text{F})$ , respectively. The infrared spectrum of this compound shows absorption bands at  $2160$  vs,  $780$  m,  $480$  m and  $290$  m  $\text{cm}^{-1}$ , which are identified as  $\nu(\text{CN}), \nu(\text{CS}), \delta(\text{NCS})$  and  $\nu(\text{Ni-NCS})$  modes, respectively, due to coordinated thiocyanate groups. Their frequencies are in good agreement with those of similar modes in transition-metal complexes which have only bridging thiocyanate groups [2, 12, 13]. The infrared spectrum is also consistent with the presence of bridging morpholine in the structure (see below). Accordingly, we suggest a six-coordinate, polymeric tetragonal configuration ( $\text{D}_{2h}$  symmetry) involving both bridging NCS and bridging morpholine for  $\text{Ni}(\text{NCS})_2\text{M}$ .

The characteristic infrared bands of morpholine in these complexes are collected in Table 4. For comparison, bands of the free ligand are also shown [14]. In liquid

Table 4 IR bands of free and coordinated morpholine

Free morpholine [14]	Ni1 <sub>2</sub> 3M (a)	Ni1 <sub>2</sub> 1.5M (a)	Ni(CN) <sub>2</sub> 1.5M (b)	Ni(CN) <sub>2</sub> M	Ni(CN) <sub>2</sub> 0.5M	Ni(NCS) <sub>2</sub> M
$\nu_1$ (3336s) (NH str)			3330m			
3298s		3180m	3300m	3300w	3300m	
			3260m	3230m		3230ww
$\nu_{30}$ 1319s	1305vs, br	1315sh	1320s	1315s	1315s	1310s
		1305s	1310s		1295s	1300s
			1290m	1285sh	1290s	
$\nu_{12}$ 1248s		1255s				
		1250s	1250m	1250s	1250s	1250s
$\nu_{31}$ 1225m (CN str)	1220s	1220s	1220w			
$\nu_{32}$ 1201m (CO str)		1200m				
		1190m	1195w	1190m		
	1185m	1185m	1170m	1165s	1170m	1170m
$\nu_{34}$ 1108vs			1120s	1120s	1120s	
		1115s	1115sh			
$\nu_{13}$ 1097vs (CN str)	1095vs, br	1100vs	1100s	1100s		
		1090s	1085s	1085s	1090m	1085s
		1085sh			1075vs	
(1062m)		1060s	1065m	1065m		
1036m (combination)	1040s	1045s	1040m	1040m	1055s	1040m
		1035s			1035m	
$\nu_{14}$ 1031 (CO str)	1030s	1030s	1030m	1030s		
		1020s			1020m	1020s
1010w		1010sh	1000m		1000w	1010s
			980m	980s	980m	
$\nu_{37}$ 891m		895m	890sh		895w	900m
884 (combination)	885s	880s	880vs	880vs, br	880sh	880vs
$\nu_{16}$ 850s, sh	875s	879vs	879vs		870vs	
	865s	865vs				
$\nu_{18}$ 595s		640m	625s	635m	640w	640m
	590s	590m	600m	620m	615s	
$\nu_{19}$ 440m	435s	435s	(c)	(c)	(c)	
$\nu_{20}$ 414w	410s, br	410s, br				
$\nu_{21}$ 268m			285sh			285m, br
			275s	270s	270s	

(a) In this compound an additional band is observed at  $\approx 1550 \text{ cm}^{-1}$ .

(b) Two small peaks are found at  $3620$  and  $1600 \text{ cm}^{-1}$  owing to traces of  $\text{H}_2\text{O}$  in the compound.

(c) This region is masked by strong absorption from  $\delta(\text{NiCN})$ .

Values in parentheses are from the equatorial conformer [14].

morpholine, the NH stretching vibrations occur at 3336 and 3300  $\text{cm}^{-1}$ ; on complexation these bands are shifted to lower frequencies, the lowest shifts being observed for the  $\text{Ni}(\text{CN})_2$ -morpholine compounds. However, in  $\text{Ni}(\text{CN})_2 \cdot 1.5\text{M}$  an additional band is observed at 3330  $\text{cm}^{-1}$ , which can be attributed to the presence of uncoordinated morpholine. In free morpholine the fundamentals  $\nu_{13}$  and  $\nu_{31}$  (at 1097 and 1225  $\text{cm}^{-1}$ , respectively) have the largest contributions from the CN stretch, whereas  $\nu_{14}$  and  $\nu_{32}$  (at 1031 and 1201  $\text{cm}^{-1}$ , respectively) are predominantly CO stretch. On this basis, the bands at 1220 and 1100  $\text{cm}^{-1}$  are assigned as derived from the fundamentals  $\nu_{31}$  and  $\nu_{13}$  of morpholine, respectively. In the range 1100–1075  $\text{cm}^{-1}$  one or two bands are observed which can be derived from  $\nu_{13}$ , since the C–N vibration will be affected by the nitrogen to nickel bonding. In  $\text{Ni}_2\text{3M}$ ,  $\text{Ni}(\text{CN})_2 \cdot 1.5\text{M}$  and  $\text{Ni}(\text{CN})_2\text{M}$  the C–O stretching mode (at 1030  $\text{cm}^{-1}$ ) is observed at the same frequency as in free morpholine, indicating that the neutral ligand acts here as a unidentate N-donor ligand. The spectra of  $\text{Ni}(\text{CN})_2 \cdot 0.5\text{M}$  and  $\text{Ni}(\text{NCS})_2\text{M}$  also show a single band at 1020  $\text{cm}^{-1}$  (i.e. 10  $\text{cm}^{-1}$  lower than in free morpholine), which can be attributed to coordination from the oxygen end of morpholine, which therefore acts as a bidentate ligand. However,  $\text{Ni}_2 \cdot 1.5\text{M}$  gives two bands, at 1030 and 1020  $\text{cm}^{-1}$ , for the C–O stretching mode, indicating the presence of both unidentate and bidentate morpholine.

#### *Reaction enthalpies*

The calibration coefficient was determined by using the expression  $\Delta Hm = KA$  [15], where  $\Delta H$  is the specific heat of transition (or reaction),  $m$  is the mass of reactive sample,  $K$  is the calibration coefficient, and  $A$  is the curve peak area. The standards used for calibration were benzophenone, benzoic acid, potassium nitrate, silver nitrate, potassium thiocyanate and sodium nitrate; the values obtained for  $K$  were in the range 3.01–4.39  $\text{J cm}^{-2}$ .

Reaction enthalpies ( $\Delta H_R$ ,  $\text{kJ mol}^{-1}$ ) for the decomposition reactions were derived from the peak areas of the endotherms via the relationship  $\Delta H_R = KAM/m$ , where  $M$  is the molar mass of the compound and the remaining terms are as defined above. Table 5 lists the results obtained for the compounds studied. For comparison, the enthalpies have also been referred to one mol of morpholine. It should be noted that, for comparable compounds, the reaction enthalpy (which is indicative of the metal-ligand bond energy) decreases as the anion size increases. The high value observed for the decomposition of  $\text{Ni}_2 \cdot 4\text{M}$  is attributed to the overlapping of the decomposition with the fusion. In the  $\text{Ni}(\text{CN})_2$ -morpholine system the enthalpy increases as the morpholine content decreases; this trend is in agreement with the above-suggested presence of free, monodentate and bidentate morpholine in these compounds.

#### *Determination of kinetic parameters*

Thermogravimetry and differential thermal analysis have been used widely to study the kinetics of thermal decomposition reactions. Sestak [16] and others have



Table 5 Reaction enthalpies in N<sub>2</sub>

Decomposition reaction	Peak temperatures, °C		<i>T<sub>f</sub></i>	Reaction enthalpy, Δ <i>H<sub>r</sub></i>	
	<i>T<sub>i</sub></i>	<i>T<sub>max</sub></i>		kJ mol <sup>-1</sup> compound	kJ mol <sup>-1</sup> morpholine
NiBr <sub>2</sub> 3M → NiBr <sub>2</sub> 2M + M	140	172	195	53.7	53.7
NiI <sub>2</sub> 4M → NiI <sub>2</sub> 3M + M	80	110	137	74.7	74.7
NiI <sub>2</sub> 3M → NiI <sub>2</sub> 1.5M + 1.5M	140	152	198	36.3	24.2
Ni(CN) <sub>2</sub> 1.5M → Ni(CN) <sub>2</sub> M + 0.5M	90	103	158	11.3	22.5
Ni(CN) <sub>2</sub> M → Ni(CN) <sub>2</sub> 0.5M + 0.5M	185	240	260	27.9	55.8
Ni(CN) <sub>2</sub> 0.5M → Ni(CN) <sub>2</sub> + 0.5M	320	378	400	59.9	119.9
Ni(NCS) <sub>2</sub> 4M → Ni(NCS) <sub>2</sub> 2M + 2M	107	153	177	77.4	38.7
Ni(NCS) <sub>2</sub> 2M → Ni(NCS) <sub>2</sub> M + M	180	212	230	63.2	63.2

*T<sub>i</sub>*, *T<sub>max</sub>* and *T<sub>f</sub>* refer to the initial, maximum deviation and final procedural decomposition temperatures.

compared results obtained by different methods. Here we apply five different methods for evaluation of the activation energy and reaction order in the process  $\text{NiBr}_2\text{3M} \rightarrow \text{NiBr}_2\text{2M}$ : three of them (Freeman–Carroll [17], Coats–Redfern [18] and Satava [19]) are thermogravimetric and the two others (Kissinger [20] and Piloyan [21]) are based on DTA. Because of the simplicity of the Coats–Redfern method, this was chosen to study all other compounds. The Satava method is cumbersome and it is often difficult to choose between either equation, and a great dispersion of the results is generally obtained with the Freeman–Carroll method. On the other hand, methods based on DTA are generally less accurate and the Piloyan method has provided a value for  $E$  which is ca. 7.5% lower than the average.

We consider briefly the equations used. The results obtained for each compound are listed in Table 2.

1. For a reaction in which the order is unknown, the final equation derived by Coats and Redfern [18] has the form

$$\log \left[ \frac{1 - (1 - \alpha)^{1-n}}{T^2(1-n)} \right] = \log \frac{AR}{aE} \left[ 1 - \frac{2RT}{E} \right] - \frac{E}{2.3RT}$$

where  $\alpha$  is the fraction of the sample decomposed at time  $t$ , and  $a$  is the heating rate. A plot of either  $\log [1 - (1 - \alpha)]^{1-n}/T^2(1-n)$  against  $1/T$  or, where  $n = 1$ ,  $\log [-\log(1 - \alpha)]/T^2$  against  $1/T$ , should result in a straight line of slope  $-E/2.3R$  for the correct value of  $n$ . Figure 2 shows the results obtained for the compounds studied as  $Y$  is plotted versus  $1/T$ . For the simplicity of the graphs, only the curves corresponding to the value of  $n$  which gives a straight line are depicted. Values of  $E$  and  $n$  obtained by this method are shown in Table 2.

2. Freeman and Carroll [17] used the equation

$$-\frac{E}{2.3R} \Delta \left( \frac{1}{T} \right) = -n + \frac{\Delta \log \left( \frac{dw}{dt} \right)}{\Delta \log W_r}$$

where  $W_r = W_c - W$ , in which  $W_c$  is the maximum mass-loss, and  $W$  is the total loss in mass up to time  $t$ . Figure 3 shows the dependence of  $[\Delta \log(dw/dt)]/\Delta \log W_r$  on  $[\Delta(1/T)]/\Delta \log W_r$ . The order of reaction obtained is  $n = 0.4$  and the slope of this plot gives  $E = 115.9 \text{ kJ mol}^{-1}$ .

3. Deduction of the mechanism of a reaction by use of nonisothermal kinetic methods has been discussed by Satava and others. According to Satava [19], the TG trace corresponding to a heterogeneous process which proceeds with a constant increase of the temperature can be described by the equation

$$\log \frac{ZE}{Ra} = \log g(\alpha) - \log p(x) = B$$

where  $B$  depends only upon the nature of the compound studied and the heating rate, but not upon the temperature. We have used the values of  $\log p(x)$  tabulated by Zsakó [22] and those of  $\log g(\alpha)$  from Satava and Skvara [23], the symbols used

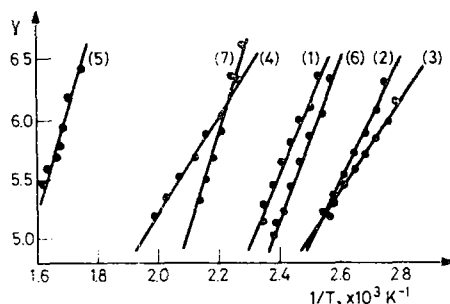


Fig. 2 Coats-Redfern plots of thermal decomposition reaction of: 1)  $\text{NiBr}_2 \cdot 3\text{M}$ ,  $n = 0.5$ ; 2)  $\text{NiI}_2 \cdot 4\text{M}$ ,  $n = 0.5$ ; 3)  $\text{Ni}(\text{CN})_2 \cdot 1.5\text{M}$ ,  $n = 0.5$ ; 4)  $\text{Ni}(\text{CN})_2 \cdot 2\text{M}$ ,  $n = 0.5$ ; 5)  $\text{Ni}(\text{CN})_2 \cdot 0.5\text{M}$ ,  $n = 0.5$ ; 6)  $\text{Ni}(\text{NCS})_2 \cdot 4\text{M}$ ,  $n = 0.5$ ; 7)  $\text{Ni}(\text{NCS})_2 \cdot 2\text{M}$ ,  $n = 1$

$$Y = -\log \left[ \frac{1 - (1 - \alpha)^{1-n}}{T^2(1-n)} \right] \text{ for } n = 0.5 \text{ and } -\log \left[ \frac{-\log(1-\alpha)}{T^2} \right] \text{ for } n = 1$$

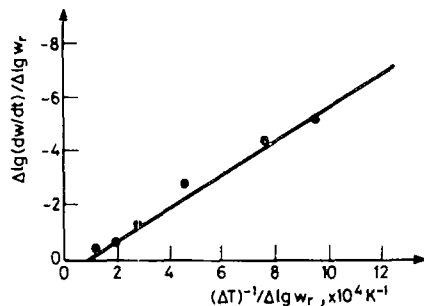


Fig. 3 Freeman-Carroll plot of thermal decomposition of  $\text{NiBr}_2 \cdot 3\text{M}$  in  $\text{N}_2$

being the same as in the paper of Sharp et al. [24]. A straight line is obtained only for the  $R_2$  function (Fig. 4). This coincides with the plot  $\log p(x)$  versus  $1/T$  for  $E = 28 \pm 0.5$  kcal ( $117 \pm 2$  kJ mol $^{-1}$ ). The result indicates that the process is controlled by a phase boundary reaction with cylindrical symmetry.

4. The plot of  $\ln T$  versus  $1/T$  presented in Fig. 5 was obtained using the equation proposed by Piloyan et al. [21]:

$$\ln T = C - \frac{E}{RT}$$

where  $C$  is a constant. It yields  $E = 105.0$  kJ mol $^{-1}$ .

5. Kissinger [20] has shown that the temperature  $T_m$  of the DTA peaks is dependent on the heating rate, according to

$$\frac{d \left| \ln \left( \frac{a}{T_m^2} \right) \right|}{d \left( \frac{1}{T_m} \right)} = -\frac{E}{R} \quad \text{where the symbols have their usual meaning.}$$

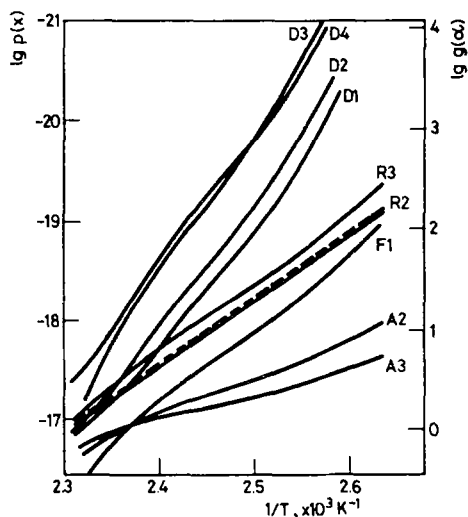


Fig. 4 Plots of  $\log g(\alpha)$  versus  $1/T_\alpha$  calculated from TG curve for various kinetic equations for  $\text{NiBr}_2\cdot 3\text{M}$

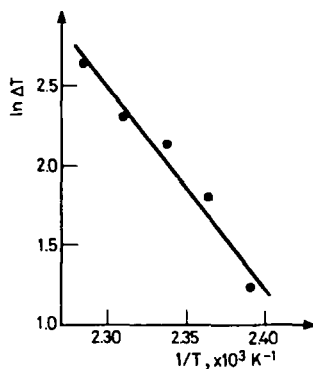


Fig. 5 Dependence of  $\ln \Delta T$  on  $1/T$  according to Piloyan for  $\text{NiBr}_2\cdot 3\text{M}$

The plot in Fig. 6, of  $\ln a/T_m^2$  versus  $1/T_m$ , gave an activation energy of  $113.7 \text{ kJ mol}^{-1}$ . By using the shape index of Kissinger for the DTA curve,  $n \sim 1.26 \text{ S}^{1/2}$ , we obtained  $n = 0.6$ .

One should note the good concordance between the results obtained for the activation energy of the process  $\text{NiBr}_2\cdot 3\text{M} \rightarrow \text{NiBr}_2\cdot 2\text{M}$  in the different methods used here. Except for the Piloyan method, the results deviate by  $\sim 3\%$  from the average. In all but one of the studied cases, the reaction orders are coincident with that obtained by the Satava method for  $\text{NiBr}_2\cdot 3\text{M}$ , i.e.  $n = 1/2$ . For this reason, the processes with  $n = 1/2$  are also suggested to be controlled by phase boundary reactions with cylindrical symmetry. According to this classification, the decomposition of  $\text{Ni}(\text{NCS})_2\cdot 2\text{M}$  ( $n = 1$ ) should be a process of random nucleation, with one nucleus on each particle.

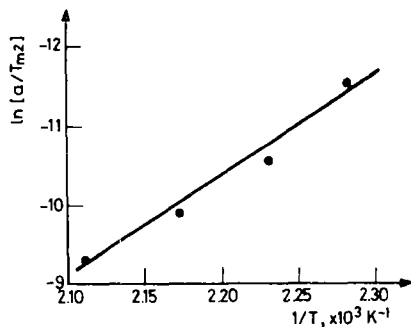


Fig. 6 Dependence of  $\ln a/Tm^2$  on  $1/T$  according to Kissinger for  $\text{NiBr}_2 \cdot 3\text{M}$

## References

- 1 J. Palazón, J. Gálvez, G. García and G. López, *Polyhedron*, 2 (1983) 1353.
- 2 I. S. Ahuja and Singh, *Transition Metal Chem.*, 2 (1977) 132.
- 3 I. S. Ahuja, *Inorg. Chim. Acta*, 3 (1969) 110.
- 4 G. Marcotrigiano, G. C. Pellacani and C. Petri, *Z. anorg. allg. Chem.*, 408 (1974) 313.
- 5 G. Schwarzenbach and H. Flashka, *Complexometric Titrations*, Methuen, London, 1969, p. 248.
- 6 B. N. Figgis and J. Lewis, in *Modern Coordination Chemistry*, Interscience Publishers Inc., New York, 1960, p. 415.
- 7 E. E. Aynsley and W. A. Campbell, *J. Chem. Soc.*, (1958) 1723.
- 8 L. Sacconi, I. Bertini and F. Mani, *Inorg. Chem.*, 6 (1967) 262.
- 9 F. A. Cotton and G. Wilkinson, *Advanced Inorganic Chemistry*, Wiley, New York, 1980, p. 790.
- 10 A. G. Sharpe, *The Chemistry of Cyano Complexes of the Transition Metals*, Academic Press, London, 1976, p. 232.
- 11 A. Ludi and R. Hugi, *Helv. Chim. Acta*, 51 (1968) 349.
- 12 S. M. Nelson and T. M. Shepherd, *J. Inorg. Nucl. Chem.*, 27 (1965) 2123.
- 13 R. J. M. Clark and C. S. Williams, *Spectrochim. Acta*, 22 (1966) 1081.
- 14 D. Vedal, O. H. Ellestad and P. Klaboe, *Spectrochim. Acta*, 32A (1976) 877.
- 15 W. W. Wendlandt, *Thermal Methods of Analysis*, Wiley, New York, 1974, p. 178.
- 16 J. Sestak, *Talanta*, 13 (1966) 567.
- 17 E. S. Freeman and B. Carroll, *J. Phys. Chem.*, 62 (1958) 394.
- 18 A. W. Coats and J. P. Redfern, *Nature*, 201 (1964) 68.
- 19 V. Satava, *Thermochim. Acta*, 2 (1971) 423.
- 20 H. E. Kissinger, *Anal. Chem.*, 29 (1957) 1702.
- 21 G. O. Piloyan, I. D. Ryabchikov, O. S. Novikova, *Nature*, 212 (1966) 1229.
- 22 J. Zsakó, *J. Phys. Chem.*, 72 (1968) 2406.
- 23 V. Satava and F. Skvara, *J. Am. Ceram. Soc.*, 52 (1969) 591.
- 24 J. H. Sharp, G. W. Brindley and B. N. Narahari Achar, *J. Am. Ceram. Soc.*, 49 (1966) 379.

**Zusammenfassung** — Die Darstellung von  $\text{Ni}(\text{CN})_2 \cdot 1.5\text{M}$  (M = Morpholin) wird beschrieben. Das thermische Verhalten dieser Verbindung und von  $\text{NiBr}_2 \cdot 3\text{M}$ ,  $\text{NiI}_2 \cdot 4\text{M}$  und  $\text{Ni}(\text{NCS})_2 \cdot 4\text{M}$  wird untersucht. Durch thermische Behandlung dieser Verbindungen werden  $\text{Ni}(\text{CN})_2 \cdot \text{M}$ ,  $\text{Ni}(\text{CN})_2 \cdot 0.5\text{M}$ ,  $\text{NiBr}_2 \cdot 2\text{M}$ ,  $\text{NiI}_2 \cdot 3\text{M}$ ,  $\text{NiI}_2 \cdot 1.5\text{M}$ ,  $\text{Ni}(\text{NCS})_2 \cdot 2\text{M}$  und  $\text{Ni}(\text{NCS})_2 \cdot \text{M}$  erhalten. Mit Ausnahme von  $\text{NiBr}_2 \cdot 2\text{M}$

und  $\text{Ni}(\text{NCS})_2\text{M}$  handelt es sich dabei um bisher noch nicht beschriebene Zwischenprodukte. Es wurden magnetische und spektrometrische Untersuchungen ausgeführt, um die Art der Koordinaten und die Stereochemie dieser Komplexe zu ermitteln. Die thermische Untersuchung erstreckt sich auf die Bestimmung der Stabilität, der scheinbaren Aktivierungsenergie und der Reaktionsordnungen sowie der Reaktionsenthalpien.

**Резюме** — Описано получение комплекса  $\text{Ni}(\text{CN})_2\text{1.5M}$  ( $\text{M}$  = морфолин), термическое исследование которого проведено совместно с комплексами  $\text{NiBr}_2\text{3M}$ ,  $\text{NiI}_2\text{4M}$ ,  $\text{Ni}(\text{NCS})_2\text{4M}$ . Термическая обработка этих комплексов приводит к образованию  $\text{Ni}(\text{CN})_2\text{M}$ ,  $\text{Ni}(\text{CN})_2\text{0.5M}$ ,  $\text{NiBr}_2\text{2M}$ ,  $\text{NiI}_2\text{3M}$ ,  $\text{NiI}_2\text{1.5M}$ ,  $\text{Ni}(\text{NCS})_2\text{2M}$ , и  $\text{Ni}(\text{NCS})_2\text{M}$ . За исключением  $\text{NiBr}_2\text{2M}$  и  $\text{Ni}(\text{NCS})_2\text{2M}$ , все остальные промежуточные соединения обнаружены впервые. С целью определения типа координации и стереохимии комплексов, было проведено исследование их магнитных и спектральных свойств. Термическое исследование включало определение их устойчивости, кажущейся энергии активации и порядков реакций, а также энтальпий реакций.